Al-Azhar Bulletin of Science

Manuscript 1678

Section: Earth science

Geochemical and petrographic Studies of Iron-ore deposits of Timsah Formation at East Aswan area, Egypt

Amr Nappout

Atef M. Hosny

Ibrahim Hashem Zidan

ORIGINAL ARTICLE – EARTH SCIENCE

Geochemical and Petrographic Studies of Iron-ore Deposits of Timsah Formation at East Aswan Area, Egypt

Amr Nappout [a,*], Atef M. Hosny [a], Ibrahim H. Zidan [b]

[a] Department of Geology, Faculty of Science, Al-Azhar University, Assiut Branch, Egypt
[b] Nuclear Materials Authority, Cairo, Egypt

Abstract

The present study concerns the Upper Cretaceous oolitic ironstones of the Timsah Formation located in East Aswan, southern Nile Valley, Egypt. The Timsah Formation contains oolitic iron ore with ~ 3–5 m thick beds. The formation is exposed along the wadi level and the lower part of the scarp face in the study area. It was subject to petrography, mineralogy, and geochemical studies to understand the genetic and characteristic features of iron-ore deposits of the Timsah Formation. The iron ooids of Aswan ironstone are suggested to be formed in sedimentary basins from land-derived iron-rich constituents. Oolitic hematitic sandstone makes up the majority of the Timsah ironstones. The hue of the oolitic ironstones might be violet, yellowish, brownish, reddish, or brownish. According to the petrographic study, the ironstones are made up of pelloids, ooids, and sometimes pisoids (pisoliths) in various forms between matrix and ferruginous cement, which is made up of clay minerals and quartz with fine to medium grains. According to radiography diffraction examination, the primary constituents of oolitic ironstone are quartz, chamosite, goethite, and hematite.

Keywords: Geochemical, Iron-ore deposits, Petrography, Timsah formation, Aswan, Egypt

1. Introduction

The iron-ore deposits have extensive occurrence in Egypt such as the Bahariya and Aswan sites. These deposits are often a link to the siliciclastic deposits (ferruginous sandstones, clays, with iron oxide bands) of deltaic and shallow marine settings. The source of the iron-ore deposits may be due to the terrestrial weathering processes and continental runoff. Several works deal with the petrography, petrophysics, and characteristic features of Nubia sandstone clastic rocks in Egypt for example [1–4]. These rocks often include more than 5% coated grains, which include pisoids, oncoids, and ooids. Van Houten [5] said that ooidal ironstones comprise mixed carbonate-siliciclastic rocks, and siliciclastic except for paleosols. Ooidal ironstones are defined as clayey, sandy, siliciclastic sedimentary, noncherty siliciclastic-carbonate or rocks that have more than 15% Fe and more than 50% ferruginous ooids, according to McGregor *et al.* [6]. Oolitic ironstones were abundant in the Ordovician, Devonian, Triassic, and Paleogene (or Jurassic-Paleogene) [7]. There was, however, a wide range of ages among them [8].

Ironstones from the Phanerozoic period are often found in shallow marine or nonmarine settings, where they are deposited as thin sequences with oolitic textures [9]. Most authors agree that chemical precipitation plays a major role in forming the concentric rings that define oolites [10]. Amorphous ferrous hydroxides are dehydrated and recrystallized, and goethite and hematite form within the fabric due to progressive diagenetic dehydration [8].

Oolitic ironstones are often found at relatively high sea-level periods when chemical weathering is made possible by a warm, humid environment [11]. Yet, it is still unclear how oolitic textures are created

Received 29 December 2023; revised 19 April 2024; accepted 10 July 2024.
Available online 18 August 2024

* Corresponding author at: Geology Department, Faculty of Science, Al-Azhar University, Assiut Branch, Assiut 71524, Egypt. Tel. +00201204444171.
E-mail address: amr112222@gmail.com (A. Nappout).

https://doi.org/10.21608/2636-3305.1678

and when hematite crystallizes in these rocks [12]. Since the Upper Cretaceous age, Conoco maps have shown the Abu Aggag [13], Timsah, Umm Brammil, and Quseir formations, and the oolitic hematite beds have been found in the Nubia sandstone sequence. Doering *et al.* [14] looked into the ironstone resources, which are located in the Wadi Abu Aggag and Wadi Subera regions northeast of Aswan, Egypt. Klitzsch [15] divided these Upper Cretaceous rocks into three units: the Um Barmil Formation (upper unit), the Timsah Formation, and the Abu Aggag Formation at the base.

The iron ore deposits occupy four horizons exposed at and above the wadi level. The iron ore four horizons occur in the Timsah Formation. The iron ore beds are more or less horizontal. The thickness of iron ore beds (oolitic iron ore) varies from 3 to 5 m in the studied area. The most economic beds of iron ore belong to the second horizon. The iron ore mainly occurs in the form of lenses and has lateral and vertical thinning. With an average iron concentration of between ~45 and 48%, the district's total ore reserves are estimated to be over 70 million tons. The country's economy will be more diversified due to the extraction of this iron ore, whose origin and surroundings have long been the topic of speculation and speculation. According to Burkhalter [16], condensate sequences deposit very slowly in moderately shallow to very shallow waters.

The present study focused on the ion-ore deposits of the Timash Formation which is located in East Aswan City. Mineralogical, petrographic, and geochemical investigations to understand the genetics, mode of occurrence, and characteristic features of iron-ore deposits of the Timsah Formation in the East Aswan region, Egypt.

2. Lithostratigraphy and geologic setting

The study area generally lies in the southern Eastern Desert (Fig. 1). The lithostratigraphy of the Upper Cretaceous in this region was subdivided into; Abu Aggag, Timsah, and Um Barmil (fluviatile-shallow marine facies, known as Nubian Sandstone), Quseir, Duwi, and Dakhla (marine facies) formations [18] (Fig. 2). This sedimentary succession unconformably overlies the Precambrian (basement) rocks. In this region, the Taref Formation was subdivided into Abu Aggag, Timsah, and Um Barmil. El-Naggar [19] confirms this subdivision and raises their stratigraphic rank to formations.

The lithostratigraphic investigation of the sedimentary sequence exposed in the study area was allowed to differentiate the following rock units [19] from base to top:

(a) Abu Aggag formation.
(b) Timsah formation.
(c) Um Barmil formation.

2.1. Abu Aggag formation

This unit occupies the lower part of the scarp face of the Nubian sandstone in the study area. It is distributed underneath the Timsah Formation and

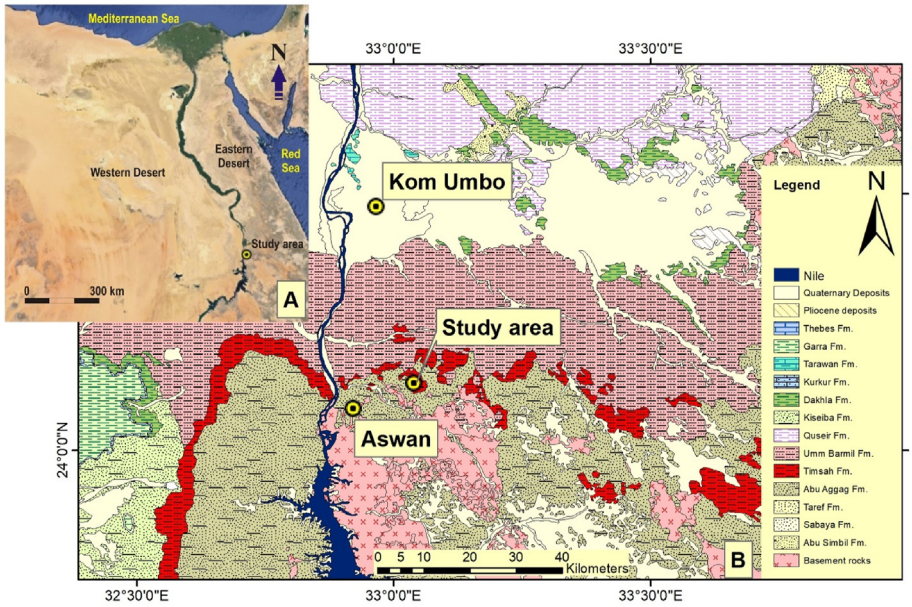

Fig. 1. a. General Google Earth image of Egypt shows the study area; b. Geologic map shows the distribution of the rock units in the Aswan region and the location of the study area (modified after [17]).

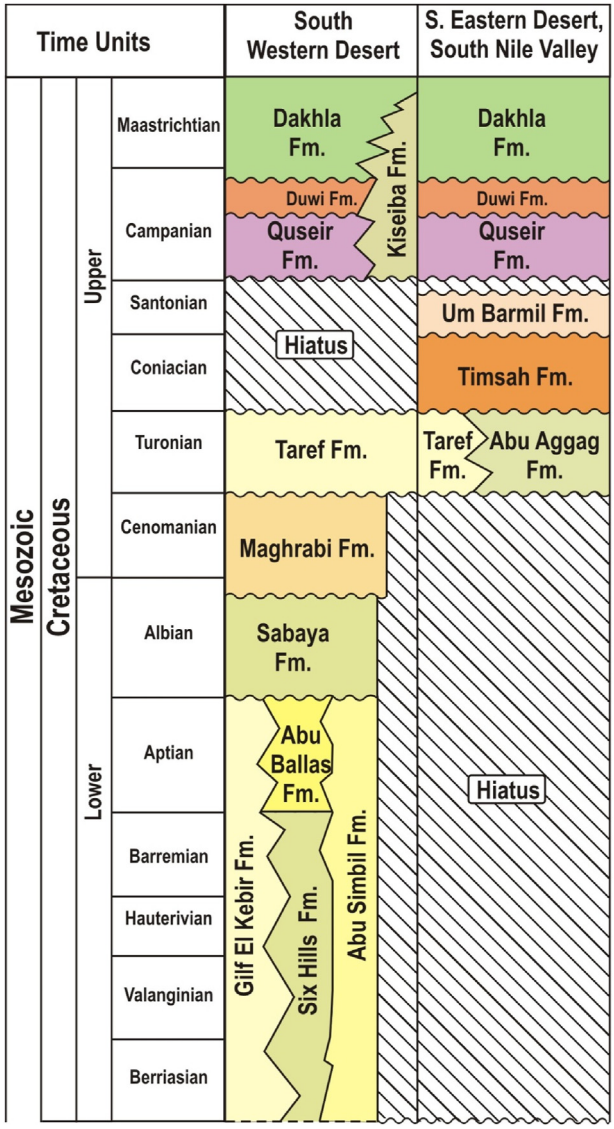

Fig. 2. General lithostratigraphic succession of the Cretaceous rocks at the south Eastern Desert and south Western Desert (modified after [18]).

occasionally free from overburden loads, especially in the areas of the exposed basement complex. The thickness of this unit ranges from a few meters to 50 m. Abu Aggag Formation consists of basal conglomerate, kaolinitic beds, clays, sandstones, and sandy clay to clayey sandstone. Clays are gray, black, reddish gray to red, clay alternated with sandstone and occasionally laterally changed into sandstone. Sandstones are gritty, coarse to fine-grained with calcareous matrix, cross-bedded (Planner and Trough), bedded alternated with iron stone, white, yellow, reddish-white, dark brown to blackish gray in parts, friable to indurated, especially in the faulted areas, concretionary with iron oxides. This unit is non-fossiliferous, but the plant remains are present in the cross-bedded sandstone and caped with a diplocraterion bank. Attia [20] gave Senonian age to this unit, while [19] gave it Turonian. Abu Aggag Formation overlies the basement complex (granite, pegmatite, schist) with irregular contact and is unconformably underlying the Timsah Formation.

2.2. Timsah formation

This formation occupies the middle part of the scarp face of the Nubia sandstone in the studied area. It unconformably overlies the Abu Aggag formation with erosional surface contact. It unconformably underlies the Um Barmil formation with marker beds (cross-bedding sandstone) and occasionally conglomeratic contact. An erosional surface mainly marks its contact with the Abu Aggag formation, while the upper contact is mainly marked by planar cross-bedding sandstone of the lower part of the Um Barmil formation. The oolitic iron ore and massive ironstone alternate, occasionally occupying many stratigraphic positions in the Timsah Formation. The iron ore occurs in 4 horizons from base to top 1, 2, 3, and 4 horizons.

The upper portion of the Nubia sandstone sequence is occupied by the Um Barmil Formation. This unit is equivalent to Taref sandstone Member in the eastern and western deserts. It is represented all over the studied area. Um Barmil Formation is ~86 m and deposited under a fluvial environment [21]. It was assigned to Santonian–Early Campanian [15,22].

3. Material and methods

The study area is located in East Aswan (Fig. 1), southern Nile Valley between longitudes 33° 2′8.56″ E and 33° 2′44.20″ E and latitudes 24° 7′56.60″ N and 24° 7′58.13″ N and covers an area of about 1.5 km^2. The study area is accessible by Cairo-Aswan roadway crossroad with Naje AL-Oshbab, which lies east of Aswan city, then going east about 21 km from the site of old Crusher that belongs to the Iron and Steel company through a dusty road. The study area lies about 25 km from Aswan City and 45 km from Aswan Airport.

A total of 40 representative samples of iron ore deposits were collected from the Timsah Formation. Ten thin-polished sections were prepared (in Assiut University lab.) and studied using a polarizing microscope in the Geologic department, Al-Azhar University (Assiut branch). The iron ore deposits of ten samples were studied using radiography diffraction (XRD) and scanning electron microscope (SEM) techniques (in Assiut University lab). Geochemical analysis of major and trace elements of

30 iron ore samples was carried out at the Nuclear Materials Authority.

4. Results and discussion

4.1. Petrography

Oolitic hematitic sandstone comprises most of the Timsah ironstones (Fig. 3). The samples of oolitic ironstone rock have a range of hues, including violet, yellowish, brownish, and reddish. They consist of ferruginous cement and matrix containing ooids (ooliths), pelloids, and seldom pisoids (pisoliths). Quartz with fine-to medium-grained particles and clay minerals comprise the matrix. The ooids are shaped differently, ranging from elliptical to spheroidal, and consist of concentric layers with different compositions around the core. The primary minerals found in these strata include chamosite, goethite, and hematite. The bulk of the cores consists of huge goethite and hematite, shattered ooids, and quartz grains, or they might be empty (or undefinable).

This study focuses on oolitic sandstone from the Timsah Formation, characterized by fine-to medium-grained quartz sand, sub-rounded to angular, and cemented by hematite. The embayed quartz is ultimately the consequence of the hematitic domains that progressively developed, corroding the quartz grains (Fig. 4a). In some thin portions of the examined oolitic ironstone, the grains are well-laminated (Fig. 4b). The majority of ironstone oolites under study have minor or subordinate elliptical forms and are spheroidal, or nicely rounded (Fig. 4a). Goethite and hematite, which are weakly differentiated in some ooids, make up the outer or concentric layers that make up the ooids. A single form of grain makes up the majority of oolites (Fig. 4c). Certain ovoidal or elliptical ooids may have concentric layers devoid of cortices or may not have cores at all (Fig. 4c). The Timsah iron stone's spheroidal or elliptical ooids are composed of various materials and have distinct forms. Certain specimens exhibit distinct cortices together with distinct core compositions and morphologies (Fig. 4d). Certain narrow portions have dense cortices and eccentric cores. Due to varying pressures and winnowing processes, some ooids have fusiform shapes; others have entire or partial cortices surrounding broken ooids.

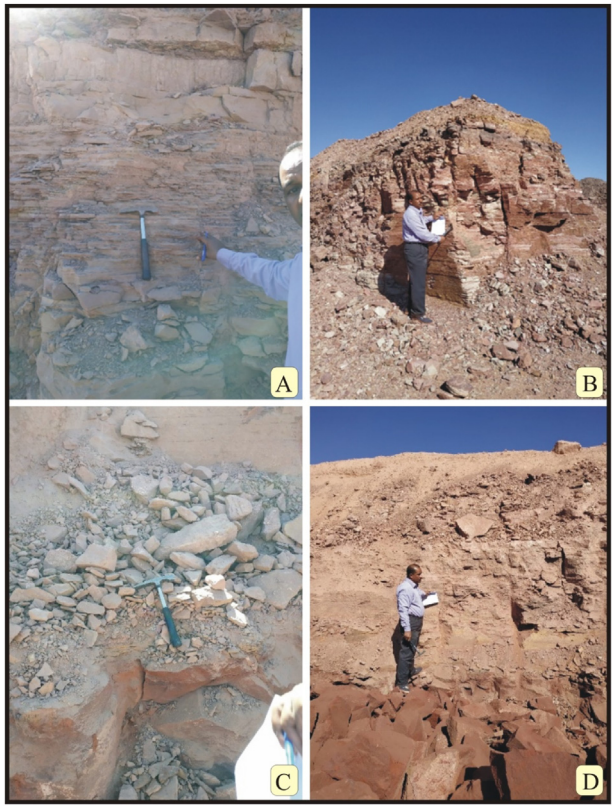

Fig. 3. Field photographs show; a, Alternating sequences in the top portion that consist of ferruginous medium-to coarse-grained; b, Oxitic reddish-brown ironstone layers; c, Oxitic ironstone bed, reddish-violet in color; d, Oolitic ironstone that ranges in color from reddish-violet at the top portion.

Certain ooids with spherical or egg-shaped shapes have undergone deformation, resulting in fractures caused by radial shrinkage and hollow cores. The ooids in quartz and hematite-goethite concrete matrixes are well-rounded. The cortices are well-defined, with a variety of ooid sizes and core compositions (Fig. 4a). Several of these ooids have asymmetric cortices, particularly the elliptical ones. Samples of well-rounded ooids have well-defined cortices with chamositic layers. In contrast, others have hematite and goethite cement layers, and some have fragments of hematite (Fig. 4d, e, and f). Compaction is the reason for some of the ooids breaking. Certain elliptical ooids have undefined or empty cores.

In contrast, others have cores made of quartz grains containing hematite iron (Fig. 4b). The Timsah iron stone's ooids experienced fragmentation and disintegration as a result of late diagenesis. The present work detected dissolved ooids in several samples, which was most likely caused by physico-chemical circumstances that caused the ooids to be etched, digested, or dissolved into the matrix. Large patches of hematite cement were produced as a consequence of the ironstone oolite grains in the matrix changing as hematitization and corrosion advanced. While some ooids are discovered as relics or fragments, others have entirely disintegrated and are now used as cementing materials.

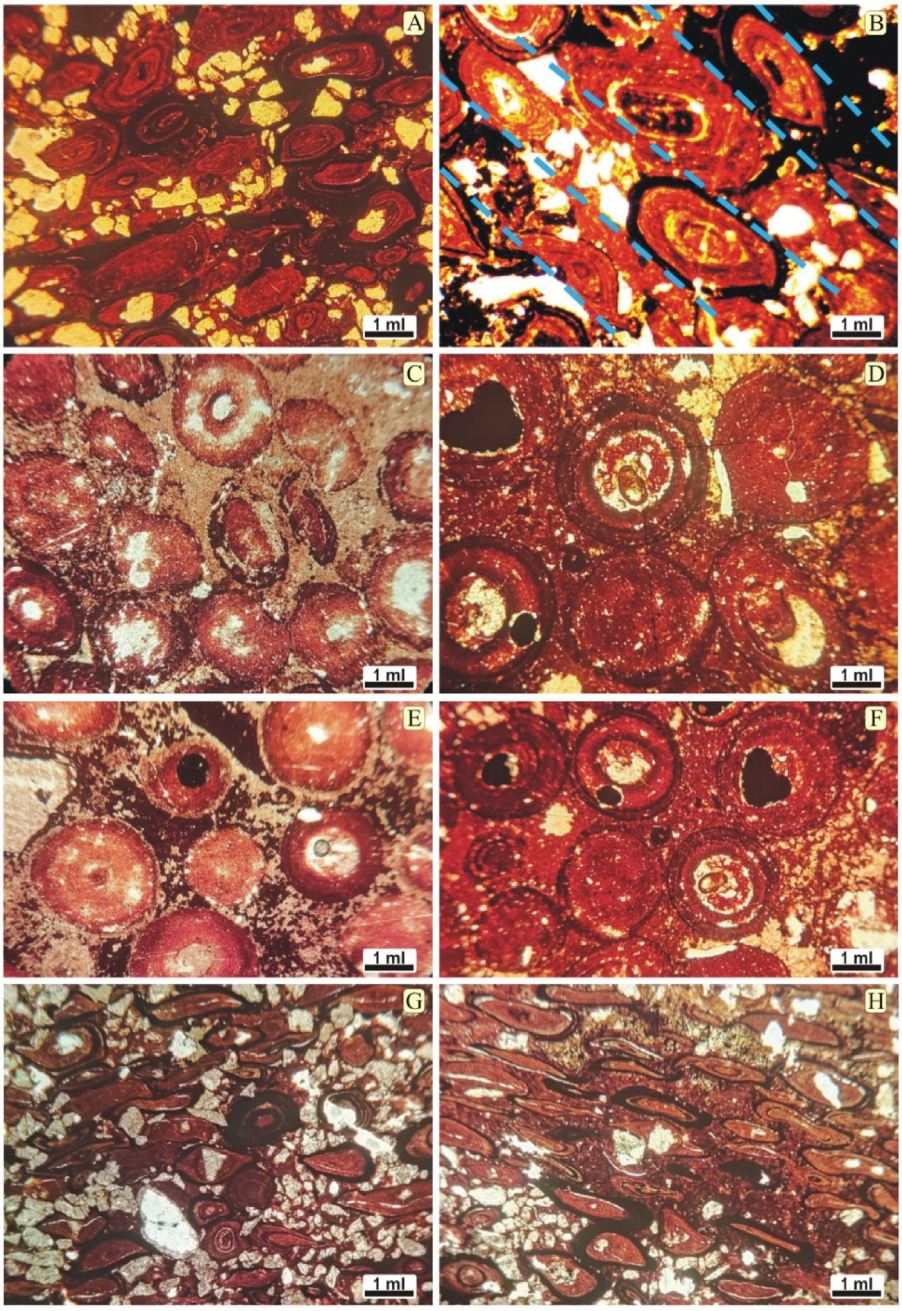

Fig. 4. Photomicrographs of Timsah Formation oolitic ironstone: (a) Oolitic sandstone displaying the latter phases of quartz grain corrosion with progressive hematitic domains (PPL, 10×). (b) Well-laminated, long oolitic ironstone (PPL, 10×) is the second kind. (c) Ovoidal ooid in micro-sprite and hematitic matrix (lacking cortex; PPL, 10×). (d, e, and f) Ooids with a well-defined cortex and a rounded shape (PPL, 10×). (f) Grain of fusiform ooid (PPL, 10×). (g and h) Compaction caused by oolitic conditions. (XPL, 10 times).

Diagenetic processes significantly influenced the development of the oolitic ironstone. In subsequent rounds of water loss, hematite, goethite, and ferrous hydroxides are formed in close association with the diagenetic recrystallization, compaction (Fig. 4g and h), and dehydration of the precursor amorphous iron-bearing clays. These processes started with creating clays stained by ferrous hydroxides.

4.2. Mineralogy

The chemical investigation of the ferruginous sandstone ore indicated the location's significant concentrations of total iron, iron oxides, and related metals. As seen in Table 1, P_2O_5 varies from 1.2 to 4.3% with uncommon levels of S and MnO, SiO_2 ranges from 7.1 to 27.2% in a reverse connection

Table 1. Chemical analysis of iron-ore deposits at East Aswan area.

S.NO.	Fe_2O_3	SiO_2	Al_2O_3	CaO	MgO	P_2O_5	MnO	TiO_2	SO_3	Na_2O	K_2O	L.O.I
1	68.5	13.5	7.2	1.3	1.6	2.1	0.3	0.7	0.2	0.2	0.1	3.9
2	70.2	12.4	6.2	1.1	1.4	1.8	0.3	0.6	0.2	0.2	0.1	3.5
3	67.3	16.2	8.5	1.5	1.9	2.5	0.4	0.9	0.2	0.2	0.1	1.5
4	65.5	16.8	8.7	1.6	1.9	2.6	0.4	0.8	0.2	0.2	0.1	1.7
5	65.7	16.5	8.6	1.5	1.8	2.5	0.3	0.8	0.2	0.2	0.1	1.8
6	58.5	18.7	10.7	2.4	2.4	3.3	0.5	1.4	0.4	0.4	0.2	1.9
7	66.2	16.3	8.5	1.6	1.8	2.5	0.4	0.8	0.2	0.2	0.1	1.5
8	48.6	23.7	15.7	2.3	2.1	22	0.7	1.8	0.5	0.5	0.2	2.1
9	47.9	24.1	14.9	3.4	3.2	2.3	0.8	1.9	0.5	0.5	0.2	1.5
10	69.2	12.6	6.7	1.2	1.5	1.9	0.4	0.6	0.2	0.2	0.1	4.5
11	66.7	15.9	8.4	1.7	1.6	2.4	0.4	0.7	0.1	0.1	0.1	2.1
12	65.8	16.7	8.8	1.5	1.8	2.6	0.3	0.8	0.2	0.2	0.1	1.9
13	59.8	18.5	9.6	2.4	2.4	2.7	0.4	1.1	0.3	0.3	0.2	2.2
14	54.2	22.2	11.7	1.8	2.5	2.9	0.5	1.5	0.4	0.4	0.2	1.9
15	58.6	19.3	10.3	2.4	2.6	2.5	0.4	1.2	0.3	0.3	0.2	1.6
16	48.2	25.1	13.2	2.3	2.9	2.9	0.7	1.7	0.5	0.5	0.2	1.3
17	44.7	27.2	13.5	2.5	3.3	3.3	0.8	1.9	0.5	0.5	0.2	1.9
18	66.3	16.2	8.5	1.6	1.8	4.3	0.4	0.8	0.2	0.2	0.1	1.2
19	67.5	15.9	8.4	1.5	1.7	2.3	0.3	0.7	0.2	0.2	0.1	1.8
20	61.4	17.6	9.1	2.2	2.7	2.4	0.5	1.3	0.3	0.3	0.2	2.1
21	66.7	15.8	8.6	1.6	1.8	2.5	0.4	0.8	0.2	0.2	0.1	1.3
22	64.3	16.7	8.8	1.7	1.9	2.6	0.5	0.8	0.2	0.2	0.1	3.6
23	59.4	24.1	13.5	2.4	2.8	3.6	0.5	1.3	0.3	0.3	0.2	3.1
24	55.9	26.4	14.5	2.6	3.2	3.8	0.7	1.4	0.4	0.4	0.2	1.5
25	65.6	16.7	8.9	1.7	1.9	2.8	0.6	1.2	0.2	0.2	0.1	1.4
26	70.1	12.3	6.3	1.2	1.2	1.9	0.2	0.5	0.1	0.1	0.1	1.3
27	69.5	7.1	5.6	1.4	1.5	2.1	0.3	0.6	0.1	0.1	0.1	1.2
28	67.8	14.9	7.8	1.5	1.8	2.3	0.4	0.8	0.2	0.2	0.1	1.5
29	58.6	14.2	6.6	2.5	2.4	2.7	0.5	0.4	0.4	0.4	0.2	2.3
30	67.5	7.8	4.8	1.4	1.7	1.2	0.3	0.6	0.2	0.2	0.1	1.8
Min	44.70	7.10	4.80	1.10	1.20	1.20	0.20	0.40	0.10	0.10	0.10	1.20
Max	70.20	27.20	15.70	3.40	3.30	4.30	0.80	1.90	0.50	0.50	0.20	4.50
Ave	62.21	17.38	9.42	1.86	2.10	2.58	0.45	1.01	0.27	0.27	0.14	2.03

with Fe_2O_3, and the Fe_2O_3 content may reach up to 70%.

Goethite, hematite, quartz, and chamosite are the primary constituents of oolitic ironstone, according to XRD examination of the samples (Fig. 5). The oolitic iron ore under study included calcite and hematite. The two minerals were imaged with SEM and XRD (Fig. 6), revealing that hematite was the primary mineral in the Timsah oolitic iron ore. Hematite may be found in two different places: in the intervals between the aggregated ooids as bigger grains and extremely small grains in concentric oolitic layers (Fig. 6a−c). Many goethite forms have been discovered, such as massive or dispersed forms, spongy oolith cores, monomineral strata with concentric layers in certain ooliths, or colloidal traces. Fig. 5 shows how easy it was to identify the goethite using XRD analysis. A ferrous aluminous silicate that chemically mimics iron-rich chlorite, chamosite contains alternating tetrahedral and trioctahedral layers. Its 2:1-layer structure, with a basal spacing of 14 Å, is comparable to mica's. Its usual composition is $(Mg, Fe, Al)_6(Al,Si)_4O_{10}(OH)_8$, with iron constituting the majority, aluminum being present in smaller amounts, and silica and magnesium being somewhat more abundant than aluminum. During accumulation, chamosite ooids often exhibit concentric layers of oxidized materials, indicating increased redox potential in the bottom environment. It can be suspected that chamosite results from the reaction of ferrous iron in solution

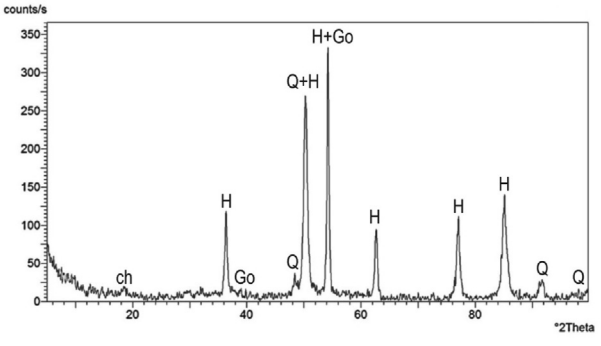

Fig. 5. Radiography diffraction pattern for representative Timsah Formation oolitic ironstone sample (Legend: ch, chamosite; H, hematite; Go, goethite; Q, quartz).

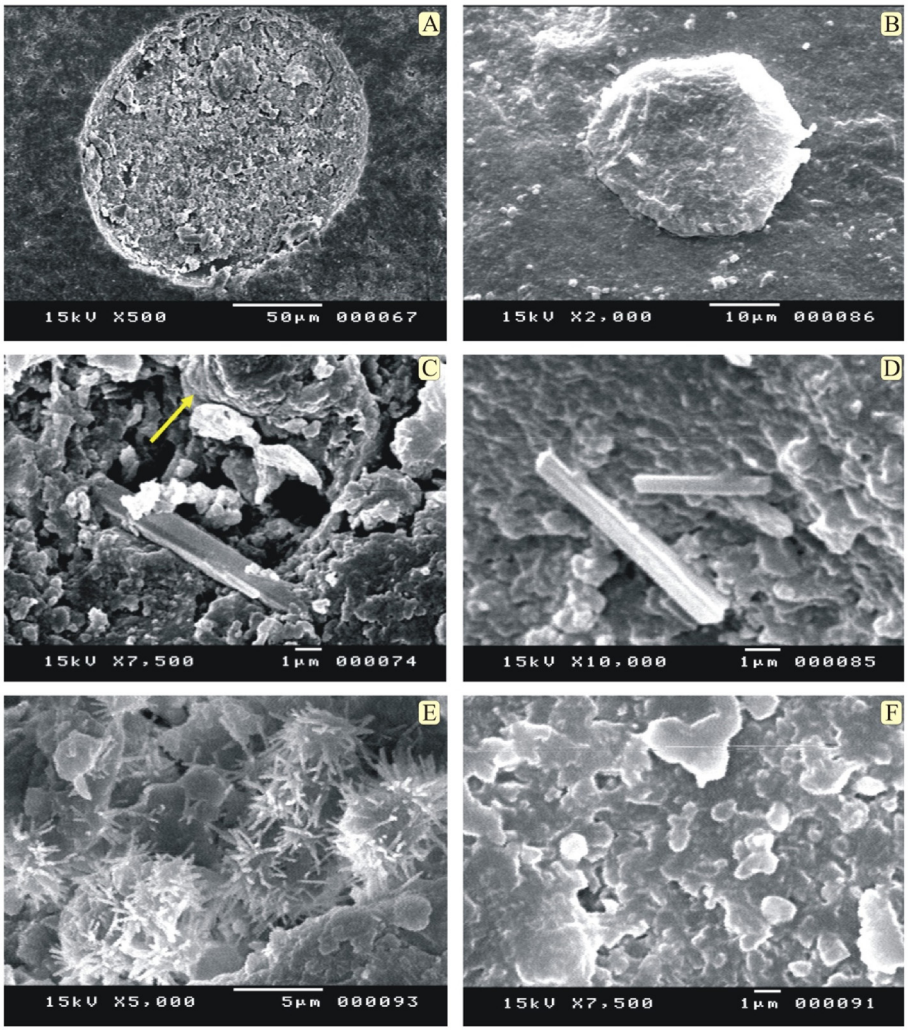

Fig. 6. Scanning electron microphotographs show (a) Ooid or ovoidal iron, (b) Ooid microtextures with layers that are concentric, (c) The cortex's hematitic makeup, (d) Cement and iron oxide particles, (e) Cementing materials and cortical microtextures, (f) Cementing materials and chamositic ooid specks.

with detrital clay particles at sea bottoms because, as predicted, its Al_2O_3 content is higher than that of other ironstone types [23]. However, the fact that chamosite replaced the clastic material suggests that the formation process included more than just clay diagenesis. The samples are accompanied by hematite-goethite minerals (SEM images and XRD). Timsah oolitic iron ore contains quartz within the ooids and between the aggregated ooids. Despite varying in size from medium-grained to extremely fine sand, most particles are fine sand.

The production of small-scale shallowing-upward cycles and sea level fluctuation (regression–transgression) coincided with the formation of oolitic ironstones during marine transgression. The ironstones are connected to quartz sandstone with fine grains, indicating that they formed on the sides of sand holes that are situated in the region where the shore-face and inner platform habitats meet [24].

It was generally accepted [25] that oolitic ironstones belonged to turbulent systems or low-energy hydrodynamic systems [26]. It has been suggested that they were either unconnected [27] or linked to sea-level variations [28]. Iron ooids have been variously interpreted as having formed at sea-level low stands [29] during transgressions [30] or at maximum-flooding surfaces [31], where changes in sea level have been suggested as a contributing factor [32] reported contemporary primary iron oxides among reef regions characterized by hydrothermal water outflow. We need to explain the first precipitated components that entered the deposition basin and the effects of the later diagenetic processes on these components before we can talk about the diagenesis of Timsah oolitic iron ore. The

dominant physico-chemical conditions (pH, organic matter content, Eh, and the concentration and level of various cations and anions in the water column and pore spaces) influence the resulting diagenetic mineral phases and associated textures. The most significant variables influencing the mineral paragenesis and textural features of Timsah ironstones nowadays are also waves and currents acting in concert with biogenic processes.

Fine-grained hematite, often found in the cortices of ooids, originally created the examined oolitic ironstones. As the ooids rolled about in turbulent seas, alumina gel and colloidal hydrohematite precipitated to cover them in consecutive concentric layers. The Timsah ironstone's red ferruginous depositional layers are thought to have been the primary source of hematite in the region, which forms the oolites. Hematite (Fe_2O_3), which was first present in unconsolidated ooids, was most likely created by secondary diagenetic processes during the conversion of Fe-rich minerals. It was thought that dehydrated sedimentary rocks generated by dehydration were mainly composed of hydrated ferric oxide precursors, like amorphous FeO−OH or goethite [33].

During diagenesis, the material transformed early ooids to hematite−chamosite ooids after their creation and consolidation. Even though its formation mechanism is poorly understood, it is thought that chamosite $(Mg, Fe)_3Fe_3(\text{-}Si_3Al)O_{10}(OH)_8$ precipitates in environments with a shift from oxic to anoxic conditions without the presence of sulfides [33]. The in-situ peloids are oolitized (by tangential expansion of ferrous hydroxides) and pseudo-ooids are formed in the last steps of dehydration and recrystallization of the ferrous hydroxides with a reddish brown color. The outcomes of the many techniques used in the research field provide intriguing insights into the potential for finding new, exploitable iron deposits in dry settings.

4.3. Conclusions

Iron prospecting is one of the main goals of geological research in Egypt's Western Desert. Ferruginous sandstones and clays are often linked to iron oxide bands. The transition from ferruginous sandstone to oolitic iron deposits is frequent. Nubian Sandstone formations, which are located unconformably on the peneplained surface of igneous and metamorphic foundation rocks, always contain sedimentary iron deposits. There is often a link between ferruginous sandstones, clays, and iron oxide bands. Iron deposits are frequently formed from ferruginous sandstone.

According to a petrographic analysis of rock samples from the Timsah Formation, the groundmass is composed largely of kaolinite, fine sand, and calcite (oolitic hematitic sandstone), with streaks of fine-grained sandstone rich in Fe_2O_3 (Fig. 6d). We came to the following conclusions based on information from petrographic and mineralogical investigations as well as field observations of the Timsah Formation:

(a) During the last phases of recrystallization and dehydration, the ferrous hydroxides laminae produced underwent full hematitization, and black peloids with a slight oolitic structure developed.
(b) Hematite and goethite were obtained by re-crystallizing amorphous ferrous hydroxides during extended periods of advanced hematitization.
(c) They were formed simultaneously as chamosite and hematite, despite hematite replacing chamosite.
(d) The ooids underwent transformation and dissolution, and late diagenetic processes formed the hematitic-goethite cement.
(e) The findings of the chemical analysis for iron oxide concentration and the intense ferrugination confirm that the examined area is a good candidate for additional in-depth geological field study and iron deposit investigation.

Conflicts of interest

There are no conflicts of interest.

Ethics information

This paper applied all the publication ethics.

Funding

There is no funders.

Author contribution

All authors planned and designed all stages of this study.

Acknowledgments

The authors would like to express their gratitude to the Geology Department of the Faculty of Science at Al-Azhar University (Assuit Branch).

References

[1] Said R. The geology of Egypt. Amsterdam: Elsevier Pub. Co.; 1962. p. 218−87.

[2] Nabawy BS, Rochette P, Géraud Y. Petrophysical and magnetic pore network anisotropy of some cretaceous sandstone from Tushka Basin, Egypt. Geophys J Int 2009;177:43−61.
[3] Nabawy BS, Géraud Y, Rochette P, Bur N. Pore-throat characterization in highly porous and permeable sandstones. Am Assoc Pet Geolog Bull 2009;93:719−39.
[4] Nabawy BS, Rochette P, Géraud Y. Electric pore fabric of the Nubia sandstones in south Egypt: Characterization and modelling. Geophys J Int 2010;183:681−94.
[5] Van Houten FB. Review of Cenozoic ooidal ironstones. Sediment Geol 1992;78:101−10.
[6] McGregor F, Ramanaidou E, Wells M. Phanerozoic ooidal ironstone deposits generation of potential exploration targets. B Appl Earth Sci 2010;119:60−4.
[7] Flügel E, Munnecke A. Microfacies of carbonate rocks: analysis, interpretation and application. Berlin: Springer; 2010.
[8] Galmed MA, Abuamarah BA, Ghrefat HA, Al-Zahrani AA. Petrology of oolitic ironstones of ashumaysi formation of wadi fatima, western Arabian Shield, Saudi Arabia. J King Saud Univ Sci 2021;33:101266.
[9] Taylor KG. Non-marine oolitic ironstones in the lower cretaceous wealden sediments of southeast England. Geol Mag 1992;129:349−58.
[10] Yoshida M, Khan IH, Ahmad MN. Remanent magnetization of oolitic ironstone beds, Hazara area, Lesser Himalayan thrust zone, Northern Pakistan: its acquisition, timing, and paleoenvironmental implications. Earth Planets Space 1998; 50:733−44.
[11] Guilbert JM, Park Jr CF. The geology of ore deposits. Waveland Press; 2007.
[12] Kimberley MM. Debate about ironstone: has solute supply been surficial weathering, hydrothermal convection, or exhalation of deep fluids? Terra Nova 1994;6:116−32.
[13] Geologic map of Egypt. Egyptian general authority for petroleum (UNESCO joint map project). Scale (1:500,000) sheet No. NH 36 SW. Conoco: Beni Suef; 1987.
[14] Doering PH, Oviatt CA, Kelly JR. The effects of the filter-feeding clam Mercenaria mercenaria on carbon cycling in experimental marine mesocosms. J Mar Res 1986;44:839−61.
[15] Klitzsch E. Plate tectonics and cratonal geology in northeast Africa (Egypt/Sudan). Geol Rundsch 1986;75:753−68.
[16] Burkhalter RM. Ooidal ironstones and ferruginous microbialites: origin and relation to sequence stratigraphy (Aalenian and Bajocian, Swiss Jura mountains). Sedimentology 1995;42:57−74.
[17] Conoco. Geologic map of Egypt. Egyptian General Authority for Petroleum (UNESCO Joint Map Project). Scale 1987;(1: 500,000).
[18] Obaidalla NA, Mahfouz KH, Metwally AA. Mesozoic sedimentary succession in Egypt. In: Hamimi Z, et al., editors. The phanerozoic geology and natural resources of Egypt, advances in science, technology & innovation. Nature Switzerland: Springer; 2023. p. 169−219.
[19] El-Naggar ZR. On a proposed lithostratigraphic subdivision for the late cretaceous-early Paleogene succession in the Nile Valley, Egypt. In7th Arab Petroleum Congress, Kuwait 1970; 64:1−50.
[20] Attia MI. Topography, geology and iron-ore deposits of the district east of Aswan. Editions universitaires d'Egypte; 1955.
[21] Kerdany MT, Cherif OH. Mesozoic. In R. Said (Ed.), The geology of Egypt 1990 (pp. 407−438). A.A. Balkema.
[22] Hendriks F, Luger P, Bovitz J, Kallenbach H. Evolution of the depositional environments of SE Egypt during the cretaceous and lower tertiary. Berliner Geowissenschaftliche Abhandlungen 1987;75(A):49−82.
[23] Rude PD, Aller RC. Early diagenetic alteration of lateritic particle coatings in Amazon continental shelf sediment. J Sediment Res 1989;59:704−16.
[24] Spalletti LA. An iron-bearing wave-dominated siliciclastic shelf: facies analysis and palaeogeographic implications (Silurian-Lower Devonian Sierra Grande Formation, Southern Argentina). Geol J 1993;28:137−48.
[25] Gygi RA. Oolitic Iron formations: marine or not marine. 1993.
[26] Ferretti A. Ooidal ironstones and laminated ferruginous deposits from the Silurian of the Carnic Alps, Austria. Bollettino della Società Paleontol Ital 2005;44:263−78.
[27] James JRHE, Van Houten FB. Miocene goethitic and chamositic oolites, northeastern Colombia. Sedimentology 1979; 26:125−33.
[28] Young TP. Phanerozoic ironstones: an introduction and review. In: Geol Soc Spec Publ. 46. London: Spe Publ; 1989. ix−xxv.
[29] Madon MB. Depositional setting and origin of berthierine oolitic ironstones in the lower Miocene Terengganu Shale, Tenggol Arch, offshore peninsular Malaysia. J Sediment Res 1992;62:899−916.
[30] Taylor KG, Simo JA, Yocum D, Leckie DA. Stratigraphic significance of ooidal ironstones from the cretaceous western interior seaway: the peace river formation, Alberta, Canada, and the castlegate sandstone, Utah, USA. J Sediment Res 2002;72:316−27.
[31] Young TP. Ooidal ironstones from ordovician gondwana: a review. Palaeogeogr Palaeoclimatol Palaeoecol 1992;99: 321−47.
[32] Heikoop JM, Tsujita CJ, Risk MJ, Tomascik T, Mah AJ. Modern iron ooids from a shallow-marine volcanic setting: mahengetang, Indonesia. Geology 1996;24:759−62.
[33] Tucker ME. Sequence stratigraphy of carbonate-evaporite basins: models and application to the Upper Permian (Zechstein) of northeast England and adjoining North Sea. J Geol Soc London 1991;148:1019−36.